Pressure-Induced Crossover from Good to Poor Solvent Behavior for Polyethylene Oxide in Water

Richard L. Cook,[a] H. E. King, Jr.,[b] and Dennis G. Peiffer
Exxon Research and Engineering Co., Corporate Research Science Laboratories, Route 22 East, Clinton Township, Annandale, New Jersey 08801
(Received 24 August 1992)

The application of pressure to solutions of polyethylene oxide in water causes phase separation through spinodal decomposition similar to that observed when the temperature is raised above the lower critical solution temperature. This phase separation pressure is dependent on molecular weight but independent of concentration. Viscosity measurements indicate a continuous decrease in the radius of gyration from good to theta solvent conditions as pressure is increased. This pressure-induced loss of solvent quality is a result of the loss of the ability of water to form hydrogen bonds at high pressure and the resulting changes in hydrophobic interactions.

PACS numbers: 61.25.Hq, 64.75.+g, 35.20.Gs, 87.15.−v

Understanding the configuration of macromolecules in water-based solutions is fundamental to many technologies as well as to much of biology. Because of the presence of electrostatic, dipole, and hydrophobic interactions as well as hydrogen bonding the conformation of aqueous polymers can show additional complexity typically not seen in nonaqueous polymers. An example of how these forces can influence configuration is given in living organisms where the cooperative effect of these interactions produces quite specific polymer chain configurations, and the resulting secondary and tertiary structures (which are known to change under pressure) [1] are responsible for a biomacromolecule's activity. The solution properties of polyethylene oxide (PEO) allow the examination of two of these forces, hydrogen bonding and hydrophobic interactions, without complications from the myriad interactions arising from multifunctional biomolecules. Nevertheless, PEO in water shows complex solution behavior manifested in its unusual phase behavior, a closed-loop temperature-concentration phase diagram at low molecular weight and a lower critical solution temperature ($\approx 100\,^{\circ}$C) for longer chain length [2]. This has attracted recent theoretical interest [3,4]. In addition, the solution behavior of PEO itself leads to many technical applications [5] including its use as a drag reducer.

Under ambient conditions PEO in water is in several ways a typical example of a polymer good solvent system. The random coil nature of PEO in water has recently been unambiguously demonstrated [6]. For example, the scaling exponents $R_g \propto M^{0.583}$, $R_h \propto M^{0.571}$, and $A_2 \propto M^{-0.20}$ are all found to be in excellent agreement with theoretical predictions for polymers in good solvents [7]. One unusual feature of PEO in water is that the second osmotic virial coefficient A_2 is unusually large, reflecting an anomalous swelling of the chains [7,8]. This is attributed to the strong water-PEO interaction through hydrogen bonding. An ambient-temperature hydration number of 2–3 water molecules per PEO monomer unit has been reported [9–11]. This unusually strong hydrogen bonding plays a pivotal role in the water solubility of PEO; for example, the structurally similar polypropylene oxide has relatively weaker hydrogen bonding and thus is insoluble in water [12]. The effect of elevated temperature is to weaken this PEO-water bonding, and this, coupled with entropic effects, is predicted to lead to a complex temperature-concentration phase diagram [3].

High-pressure studies can in general be quite revealing about such water-based systems. The major effect of pressure is to reduce the degree of hydrogen bonding in water [13–16]. The application of pressure to water is also known to diminish the strength of hydrophobic interactions [17,18]. As these are the two types of interactions that control PEO solubility, one can anticipate that high pressures can strongly perturb the solution behavior of PEO in water. In contrast, good solvent polymer solutions typically show rather small effects at high pressures. Solvent quality and thus chain dimensions may change with pressure [19], but this is usually a small ($< 20\%$) effect seen in the poor solvent regime. In a recent study of four good solvent systems it was shown that the size of the macromolecular coils was unaffected by pressures of up to 20 kbar (1 kbar = 1000 atm) [20]. Pressure is also known to affect the solubility and compatibility of polymers: While the upper critical solution temperature (UCST) may be raised or lowered by high pressure, the lower critical solution temperature (LCST) is theoretically predicted [21,22] and always observed to increase with pressure, often as much as $500\,^{\circ}$C/kbar [23–25]. As will be seen, the chain dimensions of PEO in water are quite susceptible to change under pressure and the LCST *decreases* with increasing pressure above 2 kbar.

The PEO samples were anionically polymerized with molecular weights of $M_n = 1423$, $M_w = 1489$; $M_n = 3336$, $M_w = 3662$; $M_n = 4506$, $M_w = 4948$; $M_n = 9193$, $M_w = 10904$; $M_n = 14677$, $M_w = 19683$ obtained from Pressure Chemical Co. and $M_n = 248000$, $M_w = 270000$; $M_n = 822000$, $M_w = 937500$ obtained from American Polymer Standards. The polymers were used as received and were subsequently dissolved in triply distilled water. For the $M_w = 270000$ sample, the intrinsic viscosity was experimentally determined at ambient pressure and $22.5\,^{\circ}$C in an Ubbehlode tube viscometer to be $[\eta] = 2.42 \pm 0.02$ dl/g with the Huggins coefficient 0.29

± 0.01. This value of $[\eta]$ is consistent with the known values of the radius of gyration [7] indicating the absence of aggregation in our samples.

The phase behavior was determined through studies carried out in a temperature-controlled diamond-anvil pressure cell. The phase separation temperature as a function of pressure (Fig. 1) was determined for the sample by measurement of the total transmitted light intensity through the cell at a given pressure while ramping the temperature at 0.5 °C/min. This transition is identified by an abrupt change in transmission corresponding with a microscopically visible change from a single-phase, transparent sample to a two-phase liquid mixture. The transition occurs at the same temperature to within experimental error, ± 0.2 °C, for both increasing and decreasing temperature. The pressure, determined by ruby fluorescence [26], remains constant to within experimental error, ± 0.3 kbar, in the small temperature range (typically 6 °C) of the measurement. This transition may also be observed by increasing pressure at a given temperature as is done in the determination of the molecular weight dependence (see Fig. 2). This was observed by tightening (or loosening) the pressure-controlling screws of a Merrill-Bassett diamond-anvil cell while observing microscopically the appearance (or disappearance) of phase-separated regions. In the single-phase region the viscosity of a dilute solution of PEO in water was also determined.

Upon compression above a critical pressure P_c (P_c =4.3 kbar for 1.0 g/dl and 270000 g/mol), liquid-liquid phase separation consistent with spinodal decomposition is observed. The separated regions are observed to move with Brownian motion and the system has a finite viscosity, indicating the liquid nature of the two-phase system. After a pressure jump to ca. 5 kbar at room temperature, we observe the Ostwald ripening associated with spinodal decomposition with precipitated droplets growing from an initial size of ≈ 3 to ≈ 20 μm at 1 h for this sample and similar behavior at other concentrations and molecular weights.

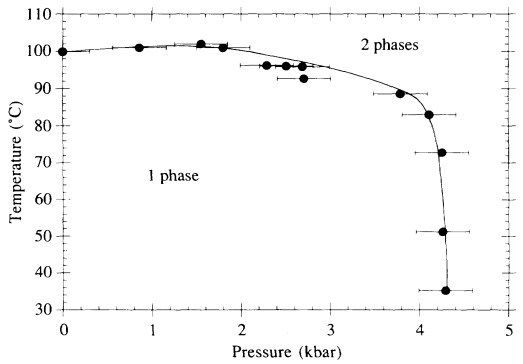

FIG. 1. Pressure-temperature phase diagram for PEO (1.0 g/dl, 270000 g/mol) in water. The system undergoes spinodal decomposition when crossing into the two-phase region upon increasing either pressure or temperature. This curve is reproducible for both increasing and decreasing pressure, indicating that the chains are not degraded by pressure.

The temperature-pressure phase diagram for one of the solutions (1.0 g/dl, 270000 g/mol) is shown in Fig. 1. At ambient pressure we see the LCST of 100 °C consistent with previous measurements [2]. Up to 1.5 kbar a slight increase in the phase-separation temperature T_c of ≈ 2 ° C/kbar is observed in agreement with the previous low-pressure data ($P \leq 0.05$ kbar) increase of 4 °C/kbar [2]. However, above 2 kbar $\partial T_c/\partial P$ becomes negative and the phase boundary becomes nearly vertical above 4 kbar. Above 4.3 ± 0.3 kbar PEO is insoluble at all temperatures.

Changes in concentration have little effect on this phase diagram. In particular, at 22.5 °C the phase separation pressure P_c for M_w =270000 g/mol is 4.35 and 4.30 ± 0.3 kbar for 1.0 and 0.3 g/dl, respectively; for M_w =19683, P_c =5.57 and 5.39 ± 0.3 kbar for 1.0 and 20.0 g/dl. Because these concentrations span the dilute to semidilute range, we can conclude that this phase-separation behavior reflects single-chain behavior.

The phase-separation pressure at room temperature is strongly dependent on molecular weight as shown in Fig. 2. At the higher molecular weights, P_c tends to saturate while at low molecular weights there is a significant elevation of P_c with decreasing M_w. At the lowest molecular weight, 1489 g/mol, P_c exceeds the freezing pressure of pure water (P =9.2 kbar), and the phase transition for this solution is a complex interplay of both phase separation and ice-VI formation. The formula for the Flory interaction parameter χ_{12c} and its application to the critical temperature [27] shows the importance of the square root

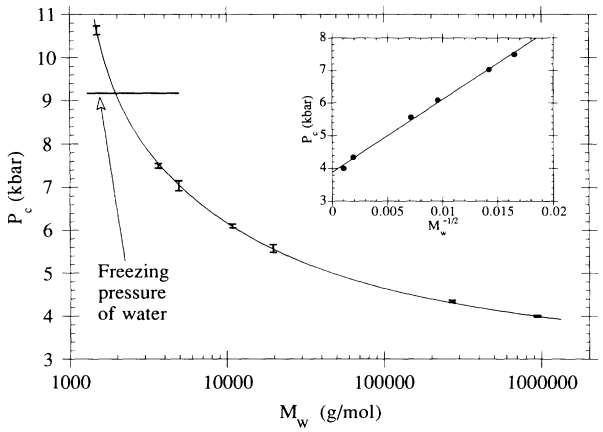

FIG. 2. Pressure–molecular-weight phase diagram of PEO in water. The curve was determined at a temperature of 22.5 ± 1 °C and at concentrations of 20 g/dl below 10^6 g/mol and 1.0 g/dl above 10^6 g/mol. Samples with $M_w \leq 1500$ g/mol remain stable in solution up to the ice-VI–liquid equilibrium pressure of water at 9.2 kbar. The limits of the error bars represent the pressures measured above and below the transition and the line serves to guide the eye. Inset: A linear relation between P_c and $M_w^{-1/2}$ as discussed in the text.

of molecular weight on phase compatibility:

$$\chi_{12c} = \tfrac{1}{2} + 1/x^{1/2}, \quad (1)$$

$$1/T_c = 1/T_\theta + kM_w^{-1/2}, \quad (2)$$

where x is the degree of polymerization. We find (see Fig. 2, inset) at 22.5 °C for samples of various molecular weight the empirical relationship

$$P_c = P\theta + k'M_w^{-1/2}. \quad (3)$$

This suggests that χ_{12c} is linearly dependent on pressure under critical conditions. In analogy with the use of a Shultz-Flory plot to calculate T_θ, the y intercept in the inset of Fig. 2 yields $P_\theta = 3.9$ kbar.

The effect upon the phase behavior of substituting D_2O for H_2O is small. We find that P_c decreases to 3.98 ± 0.3 kbar for 1.0 g/dl, 270000 g/mol solution of PEO in D_2O as opposed to 4.30 ± 0.3 kbar in H_2O. One effect of the use of D_2O is to alter the degree of hydrogen bonding, and this can be more drastically altered through the use of methanol as a solvent. Unlike PEO in water, published results suggest [28] and we observe that PEO crystallizes out of methanol solution at pressures above ≈ 2 kbar over the course of a few hours.

If the phase separation for PEO in water is considered to be arising from a deterioration of solvent quality with increasing pressure (i.e., $\partial\chi/\partial P > 0$), a significant change in chain dimensions is expected in going from swollen chains to collapsed ones. This can be calculated from viscosity data using the method of a previous study [29]. Figure 3 shows the experimental PEO solution viscosity data (upper curve) measured by the velocity of a rolling ball within the diamond-anvil cell [30]. As can be seen, viscosity actually decreases with increasing pressure, a phenomenon previously known only for water below 20 °C from 0 to 2 kbar [31].

With these data and the pressure-dependent viscosity of water [32], the viscosity radius ($R_\eta = R_g^{2/3}R_h^{1/3}$, where R_g is the radius of gyration and R_h is the hydrodynamic radius) of the PEO chain can be calculated. High-pressure intrinsic viscosity is calculated from the ratio of high-pressure solution and solvent viscosity using the Huggins equation with a Huggins coefficient of 0.29. (This calculation does not account for an increase in the Huggins coefficient one might anticipate with decreasing solvent quality as pressure rises; as such this calculation is an upper bound to the actual radius.) The radius (Fig. 4) R_η is then calculated from the Flory relationship [27] $[\eta] = \Phi' R_\eta^3 M^{-1}$, where $\Phi' = 3.7 \times 10^{22}$ dl mol^{-1} cm^{-3}.

R_η can be used to infer solvent quality. At ambient pressure, where good solvent conditions apply, R_η has been measured as 26.2 nm [7], in good agreement with our result (see Fig. 4). R_η under theta conditions has been measured as 17.0 nm in 0.45M K_2SO_4 at 35 °C [33] as 18.0 nm in diethylenglycolethyl ether at 50 °C [27], and as 18.2 nm in the melt [34]; these values compare well with our result at 4.3 kbar. Recent small-angle neutron scattering measurements on PEO in D_2O show declining values for R_g and A_2 with increasing pressure [8]. Extrapolation to $A_2 = 0$ gives a value in good agreement with the P_c found here. Thus the data of Fig. 4 may be interpreted as the chain collapsing to the theta conformation as solvent quality smoothly decreases with increasing pressure.

This drastic change in solvent quality for PEO and water at high pressure is not observed in many other polymer solvent systems, including those involving water as a solvent where electrostatic forces replace hydrogen bonding as the dominate polymer-solvent interaction (i.e., ionomers). R_η for partially hydrated polyacrylamide in water is pressure independent [20]. However, our result of decreasing radius with pressure is similar to high-temperature behavior of PEO in water. For example, the second virial coefficient of PEO in water has been found

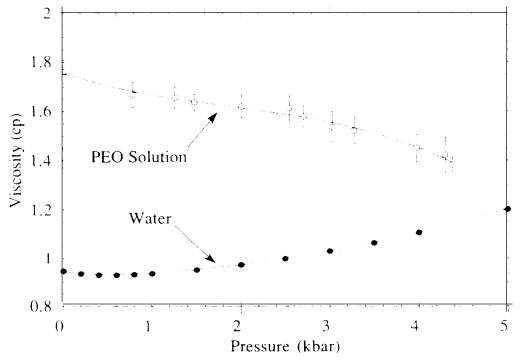

FIG. 3. Viscosity of PEO (0.3 g/dl, 270000 g/mol) in water. The water viscosity is from Bruges and Gibson [32] in quantitative agreement with measurements made in the diamond-anvil cell [30]. The decrease in viscosity with pressure for the PEO solution is a unique result known only for water below 2 kbar and 20 °C.

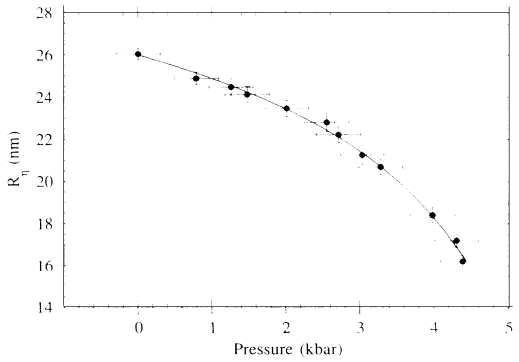

FIG. 4. Viscosity radius R_η calculated from the viscometric data of Fig. 3. The decrease in radius with pressure shows a contraction of the polymer chain from the expanded, good solvent configuration to the contracted, theta solvent conformation. Any further increase in pressure results in phase separation.

to decrease to zero at 102°C [35]. This is driven by the continuous decrease in PEO's hydration number from 2 to 3 at ambient temperature to nearly zero near T_θ [36]. Clearly this further demonstrates the importance of hydrogen bonding in promoting good solvent behavior for the PEO-water system.

The phase diagram of PEO in water is unusual in several respects. Typically the LCST of polymer systems is elevated with pressure, a fact both predicted by theory and experimentally observed [21–25]. While this is observed here up to 2 kbar, as would be expected on simple thermodynamic grounds using the Clausius-Clapeyron equation and noting that the volume of mixing is small and negative (≈ -2 cm^3/mol) and that the entropy of mixing is also negative [12], above this pressure the LCST decreases. Eventually this leads to $\partial P/\partial T_c \approx 0$, implying that at this point $\Delta S_{\text{mix}} = 0$. Clearly this is a significant change from the ambient-pressure situation. This can be associated with both the reduction in hydrophobic interactions under pressure as well as the decrease in hydrogen bond strength. These hydrophobic interaction are driven by the ordering of water, for which is paid an energy cost proportional to the entropy loss over a random arrangement of molecules. As the extent of this ordering diminishes under pressure, the entropy is expected to approach that of random mixing; in other words, crossover from the negative value at ambient pressure to a positive value at high pressure. The decrease in hydrogen bonding in water at high pressure is known through NMR diffusion measurements [13,14], and has been modeled with molecular dynamics [15,16]. This has been used to explain water's decline in viscosity with pressure [31]. We believe that this loss of hydrogen bonding ability in water at high pressure plays a major role in the pressure-induced deterioration of solvent quality.

We would like to express our appreciation to P. Pincus, W. Graessley, C. Herbst, W. Li, and D. Herschbach for their many helpful suggestions as well as to M. Rabeony for use of his laboratory and expertise.

---

[a]Present address: Department of Chemistry, Harvard University, Cambridge, MA 02138.

[b]To whom correspondence should be addressed.

[1] Y. Taniguchi and N. Takeda, in "Pressure-Induced Secondary Structure of Proteins Studied by FT-IR Spectroscopy," Proceedings of the First European Seminar of High Pressure and Biotechnology, Montepelie, 1992 (to be published).

[2] S. Saeki, N. Kuwahara, M. Nakata, and M. Kaneko, Polymer **17**, 685 (1976).

[3] A. Matsuyama and F. Tanaka, Phys. Rev. Lett. **65**, 341 (1990).

[4] P. G. de Gennes, C. R. Acad. Sci. Ser. 2 **313**, 1117 (1991).

[5] N. Clinton and P. Matlock, in *Encyclopedia of Polymer Science and Engineering*, edited by H. F. Mark, N. B. Bikales, C. G. Overgerger, and G. Menges (Wiley, New York, 1986), 2nd ed. Vol. 6, p. 242.

[6] K. Devanand and J. C. Selser, Nature (London) **343**, 739 (1990).

[7] K. Devanand and J. C. Selser, Macromolecules **24**, 5943 (1991).

[8] N. Vennemann, M. D. Lechner, and R. C. Oberthür, Polymer **28**, 1738 (1987).

[9] N. B. Graham, M. Zulfiqar, N. E. Mwachuku, and A. Rashid, Polymer **30**, 528 (1989).

[10] K.-J. Liu and J. L. Parsons, Macromolecules **2**, 529 (1969).

[11] W. Bell and R. A. Pethrick, Eur. Polym. J. **8**, 927 (1972).

[12] R. Kjellander and E. Florin, J. Chem. Soc. Faraday Trans. 1 **77**, 2053 (1981).

[13] D. J. Wilbur, T. DeFries, and J. Jonas, J. Chem. Phys. **65**, 1783 (1976).

[14] J. Jonas, T. DeFries, and D. J. Wilbur, J. Chem. Phys. **65**, 582 (1976).

[15] G. Pálinkás, Z. Naturforsch. **39a**, 179 (1984).

[16] F. H. Stillinger and A. Rahman, J. Chem. Phys. **61**, 4973 (1974).

[17] N. Nishikido, M. Shinozaki, G. Sugihara, and M. Tanaka, J. Colloid Interface Sci. **74**, 474 (1980).

[18] M. Tanaka, S. Kaneshina, K. Shin-No, T. Olajima, and T. Tomida, J. Colloid Interface Sci. **46**, 132 (1974).

[19] N. Schott, B. Will, and B. A. Wolf, Makromol. Chem. **189**, 2067 (1988).

[20] R. L. Cook, H. E. King, Jr., and D. G. Peiffer, Macromolecules **25**, 2928 (1992).

[21] I. C. Sanchez, in *Polymer Compatibility and Incompatibility*, edited by K. Solc (MMI Press, New York, 1982), pp. 59–76.

[22] D. Patterson and A. Robard, Macromolecules **11**, 690 (1978).

[23] L. Zeman and D. Patterson, J. Phys. Chem. **76**, 1214 (1972).

[24] E. Maderek, G. V. Schulz, and B. A. Wolf, Makromol. Chem. **184**, 1303 (1983).

[25] S. Rostami and D. J. Walsh, Macromolecules **18**, 1228 (1985).

[26] H. E. King, Jr., and C. T. Prewitt, Rev. Sci. Instrum. **51**, 1037 (1980).

[27] P. J. Flory, *Principles of Polymer Chemistry* (Cornell Univ. Press, Ithaca, NY, 1953).

[28] B. Nyström, K. Olafsen, and J. Roots, Polymer **32**, 904 (1991).

[29] R. L. Cook, H. E. King, Jr., and D. G. Peiffer, Macromolecules **25**, 629 (1992).

[30] H. E. King, Jr., E. Herbolzheimer, and R. L. Cook, J. Appl. Phys. **71**, 2071 (1992).

[31] P. W. Bridgman, Proc. Am. Acad. Arts. Sci. **61**, 57 (1926).

[32] E. A. Bruges and M. R. Gibson, J. Mech. Eng. Sci. **11**, 189 (1969).

[33] F. E. Bailey, Jr., and R. W. Callard, J. Appl. Polym. Sci. **1**, 56 (1959).

[34] G. D. Wignall, L. Mandelkern, C. Edwards, and M. Glotin, J. Polym. Sci. Polym. Phys. Ed. **20**, 245 (1982).

[35] W. F. Polik and W. Burchard, Macromolecules **16**, 978 (1983).

[36] B. P. Makogon and T. A. Bondarenko, Polym. Sci. USSR **27**, 630 (1986).